Reconstructing Karcher Means of Shapes on a Riemannian Manifold of Metrics and Curvatures

Boris A. Gutman[1], P. Thomas Fletcher[2], Greg Fleishman[3], Paul M. Thompson[1]

1. Imaging Genetics Center, INI, KSOM, University of Southern California
2. School of Computing, University of Utah
3. Department of Bioengineering, University of California Los Angeles

Abstract. In a recent paper [1], the authors suggest a novel Riemannian framework for comparing shapes. In this framework, a simple closed surface is represented by a field of metric tensors and curvatures. A product Riemannian metric is developed based on the L^2 norm on symmetric positive definite matrices and scalar fields. Taken as a quotient space under the group of volume-preserving diffeomorphisms, the space becomes a proper metric manifold of shapes. In this work, we simplify this representation, showing that only mean curvature and metric tensor fields are needed for a complete surface representation. In this simplified framework, we develop an algorithm for computing Karcher means, and compare the results to standard Euclidean averages of surface embeddings.

Keywords: Shape Analysis, Riemannian Metric, Surface Registration, Cortical Surface, Karcher Mean

1 Introduction

Comparison of simple 3D shapes remains one of the staples of medical image analysis. As in any population analysis, statistical comparison of a group of shapes typically requires a group template, the average shape. However, computing means of shapes requires a metric which respects the invariance to Euclidean motion that is inherent in proper shape analysis. In the absence of such a metric, the mean shape is often approximated as a Euclidean average of coordinates after registration and affine alignment. Many non-linear registration tools for shapes have been developed, of which we name a few below.

Gu et al., developed a conformal mapping algorithm [2] for spherical mapping and formulated a landmark-matching energy as a Mobius transform. A relaxation of the conformal energy, the quasi-conformal mapping of Zeng et al. [3] simultaneously solves the Beltrami equations and minimizes curvature mismatch. Shi et al. [4] applies fluid registration to the flat 2D domain after conformally mapping a surface with prescribed boundaries. Spherical Demons [5] adapts the diffeomorphic demons algorithm [6] to the sphere, matching curvature-derived intensity functions to register cortical surfaces. A similar approach is taken in [7], adapting fluid registration [8] to the sphere. In [9], the authors compute high-dimensional embeddings of surfaces based on eigenfunctions of the Laplace-Beltrami Operator (LBO). In this approach, metric tensors are scaled to match the resulting LBO representations in the Euclidean sense.

A number of manifolds of shape representations are possible, see for example [10]. In general, these fall into one of two categories: metrics on spatial diffeomorphisms to be applied to a known surface embedding, and metrics on representations from which the surface can be reconstructed directly. In the first category, the authors in [11] apply the large deformation framework to compute the length of the path in the space of diffeomorphism resulting from morphing one boundary onto another. An improvement on this is suggested in [12], measuring distances on the deformation of the surface itself rather than in the ambient space as done in [11]. Using [11], the authors in [13] develop an EM approach to estimate the shape mean based on the initial momentum describing the set of deformations.

In the second category, Kurtek et al. [14] developed a Riemannian framework for simple surfaces, using q-maps. The L^2 distance on q-maps, or simply the surface embedding weighted by the root of the volume form, remains invariant under reparameterizations. Q-maps can be used to directly reconstruct the surface, a significant advantage over previous methods. Computing averages of a group of shapes reduces to estimating the mean q-map under spherical diffeomorphisms. However, the representation is still of the surface *embedding*, with all the resulting nuisances. Some standard heuristics are applied to the initial surfaces, namely centering each shape at the origin. This implies that a local change in the surface has a global effect on the representation. Further, the metric is on the space $\mathcal{S}$ of smooth functions from the 2-sphere to $\mathbb{R}^n$, which ignores the surface metric structure.

Finally, in [1] the authors proposed a metric on a surface representation which is completely independent of the surface embedding. Applying the Ebin metric to a field of pullback metric tensors on the sphere, and the L^2 metric to mean and Gaussian curvatures, the authors develop a Riemannian space of shapes. The representation can then be used to reconstruct the surface purely from intrinsic surface properties, with no need to normalize for Euclidean motion. Further, the mapping between surfaces resulting from removing the action of volumorphisms leads to an equiareal surface-to-surface mapping that is as-conformal-as-possible. Building on this framework, we make the following contributions: First, we show that the conformal equivalence between genus-zero shapes implies that the shapes can be uniquely represented with a field of spherical tensor metrics and mean curvatures, as shown in [15]. Thus, Gaussian curvature is no longer required. Second, we develop an algorithm for computing Karcher means of these representations from a population of shapes. Our modified reconstruction algorithm produces plausible reconstructed averages for subcortical and cortical surface models.

The remainder of the paper is organized as follows. Section 2 introduces the Riemannian metric on metric tensors, describing briefly its invariance properties. Section 3 describes the full metric plus curvature framework, showing that our representation is sufficient to reconstruct a surface. Section 4 shows how the framework can be used to compute intrinsic means of metric plus curvature maps. Section 5 gives some implementation aspects. Sections 6 and 7 present some experimental results and conclude the paper.

2 A Metric on Metrics

Given a set of surfaces with a mapping from the 2-sphere $\mathbb{S}^2$ to space, $\mathcal{S} = \{S: \mathbb{S}^2 \to \mathbb{R}^3 | S \in C^\infty\}$, we represent the metric structure of our shapes as the pull-back metric tensor g, $g_{i,j} = S_i^T S_j$. The field of these tensors lives in the space of positive definite tensors $\mathcal{M}(\mathbb{S}^2) = \{h: T\mathbb{S}^2 \times T\mathbb{S}^2 \to \mathbb{R} | h \in SPD(2)\}$. A metric on this space must be invariant to reparameterizations of a pair of tensor fields to be an intrinsic distance on metric structures. More formally, for a given metric on $\mathcal{M}$, the group of diffeomorphisms on $\mathbb{S}^2$ must act on $\mathcal{M}$ by isometry. Ebin et al. [16] showed that the L^2 Riemannian metric on the tangent bundle of $\mathcal{M}$, satisfies this criteria: given $g \in \mathcal{M}$, $h, k \in \Sigma \cong T_g\mathcal{M}$, the metric can be written as:

$$(h, k)_g = \int_M \langle h, k\rangle_g d\mu_g, \tag{1}$$

where $\langle h, k\rangle_g$ is the inner product induced by g, $\langle h, k\rangle_g = tr(g^{-1}hg^{-1}k)$, and μ_g is the volume form also induced by g. This metric produces geodesics on $\mathcal{M}$ whose length can be computed point-wise and in closed form. A reparameterization $\varphi \in \Phi = \{\phi: \mathbb{S}^2 \to \mathbb{S}^2 | \phi, \phi^{-1} \in C^2\}$ acts on g by conjugation with the pushforward (Jacobian)$D\varphi: T_x\mathbb{S}^2 \to T_{\varphi(x)}\mathbb{S}^2$, $\varphi \circ g = D\varphi^T g\, D\varphi$. Given two parameterized surfaces $A, B \in \mathcal{S}$, a closed-form solution for the geodesic distance between g_A and g_B at a point x is [17]

$$D(g_A[x], g_B[x]) = \sqrt{\int_0^1 \langle g_t'(x), g_t'(x)\rangle_{g_{t(x)}} dt} = \left\| \mathrm{Log}\left[g_A^{-1/2} g_B g_A^{-1/2}\right]\right\|_F. \tag{2}$$

This metric can be shown to be invariant under simultaneous spherical re-mappings of A and B [17], since $D(g_A, g_B) = D(D\varphi^T g_A D\varphi, D\varphi^T g_B D\varphi)$.

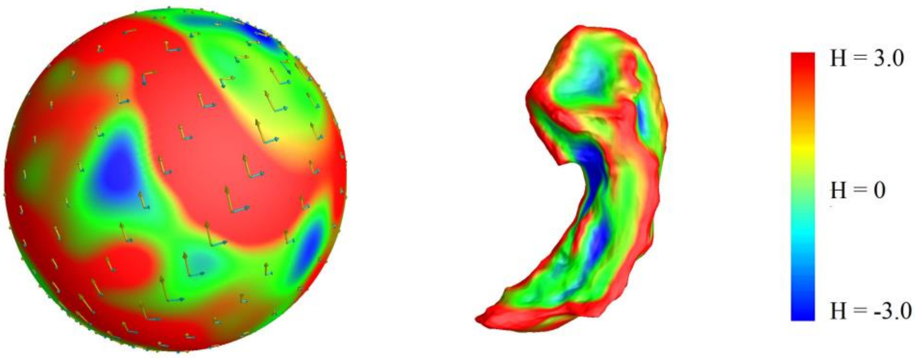

Fig. 1. Metric tensor fields and mean curvature – a complete surface representation. Tensors are displayed as their eigenvectors in $T\mathbb{S}^2$ with magnitude corresponding to the eigenvalues. The color map indicates mean curvature. The scale bar indicates mean curvature values.

3 Metrics on the Space of Surfaces

The change in the volume form due to reparameterization prevents a straightforward generalization of $(\cdot\,,\,\cdot)_g$ to the quotient space $\mathcal{M}\backslash\Phi$. Instead, the authors in [1] consider the submanifold $\mathcal{M}_\mu$ of metrics which correspond to a fixed measure μ. $\mathcal{M}_\mu$ is a metric space under $(\cdot\,,\,\cdot)_g$. The restriction of Φ to its subgroup of maps with a unitary pushforward $\Phi_U = \{\phi \in \Phi | det(D\phi) = 1\}$, leads to a quotient space $\mathcal{M}_\mu\backslash\Phi_U$ that is a metric space under the metric

$$\mathfrak{D}(A,B) = \min_{\varphi\in\Phi_U}\left(\int_{\mathbb{S}^2}\left\|\operatorname{Log}\left[g_A^{-1/2}\varphi\circ g_{\varphi\circ B}g_A^{-1/2}\right]\right\|_F^2 d\mathbb{S}^2\right)^{1/2} \quad A,B\in\mathcal{S}_1. \tag{3}$$

Here, $\mathcal{S}_1$ is the restriction of $\mathcal{S}$ to equiareal spherical parameterizations of shapes with normalized surface area.

The metric $\mathfrak{D}(A,B)$ allows us to compute intrinsic distances between metric structures. However, metric structure must be augmented with curvature information in order to represent a surface uniquely. The following theorem given by Gu, et al. [15], shows how this may be done in the case of conformal parameterization:

Theorem 1. *A closed conformally parameterized surface S in* $\mathbb{R}^3$ *is determined by its conformal factor* λ *and its mean curvature H uniquely up to Euclidean motion, where the metric tensor* $g = \lambda I$.

As our spherical parameterization is equiareal, we cannot expect them to be conformal except in the trivial case where $S = \mathbb{S}^2$. However, it is known that for all genus-zero surfaces there exists a conformal equivalence. Further, a conformal reparameterization can be found using only the metric structure, without knowing the surface [15]. Thus, we have the following result:

Theorem 2. *A closed parameterized surface* $S \in \mathcal{S}$ *is determined by its metric tensor* g *and its mean curvature H uniquely up to Euclidean motion.*

We note also that a generalization of this result is shown in [18]. An illustrative example of such a representation is shown in **Figure 1** above. From this result, it is clear that we only need augment the space $\{\mathcal{M}(\mathcal{S}_1)\backslash\Phi_U,\ \mathfrak{D}(\cdot,\cdot)\}$ with a corresponding metric on H. We now define the space of shapes as

$$\mathfrak{S} = \left\{\mathcal{M}(\mathcal{S}_1)\times C^2(\mathbb{S}^2)\backslash\Phi_U,\ \ \mathfrak{D}(\cdot,\cdot)\times D_{L^2\backslash\Phi_U}(\cdot,\cdot)\right\} \tag{4}$$

Here, $C^2(\mathbb{S}^2) = \{f\colon \mathbb{S}^2 \to \mathbb{R} | f \in C^2\}$, and the usual L^2 distance modified by Φ_U, $D_{L^2\backslash\Phi_U}(a,b) = \min_{\phi\in\Phi_U}\sqrt{\int_{\mathbb{S}^2}(a-\phi\circ b)^2 d\mathbb{S}^2}$. For brevity, we will call the 2-product metric $\mathcal{L}(\cdot,\cdot) = \mathfrak{D}(\cdot,\cdot)\times D_{L^2\backslash\Phi_U}(\cdot,\cdot)$, defined explicitly as

$$\mathcal{L}(A,B) = \sqrt{\mathfrak{D}^2(A,B) + D^2_{L^2\backslash\Phi_U}(H_A,H_B)}. \tag{5}$$

4 Computing the Karcher Mean on $\mathfrak{S}$

Given a set of parametric surfaces representations $\mathfrak{s} = \{S_i | S_i \in \mathfrak{S}\}$, we would now like to find their intrinsic average. Note that by intrinsic we mean invariant to affine transformations, i.e. in our sense mean curvature is "intrinsic." Finding the Karcher mean $\nu(\mathfrak{s}) = \{g_S, H_S\}$ under $\mathcal{L}(\cdot,\cdot)$ requires simultaneous estimation of geodesic lengths to each shape's orbit in $\mathfrak{S}$. In other words, we must find several reparameterizations $\phi_i \in \Phi_U$, while estimating $\nu(\mathfrak{s})$:

$$\nu(\mathfrak{s}) = \underset{S \in \mathfrak{S}}{\operatorname{argmin}} \left(\min_{\phi_i \in \Phi_U} \sum_i \int_{\mathbb{S}^2} \left\| \operatorname{Log}\left[g_{S_i}^{-\frac{1}{2}} \phi_i \circ g_{\phi_i \circ S} g_{S_i}^{-\frac{1}{2}} \right] \right\|_F^2 + \left[H_{S_i} - \phi_i \circ H_S \right]^2 d\mathbb{S}^2 \right) \quad (6)$$

Estimating $\nu(\mathfrak{s})$ can be done with a two-step optimization: first, holding the estimates of the ϕ_i constant to update the current $\nu(\mathfrak{s})$ estimate; and second, holding $\nu(\mathfrak{s})$ constant to update all remappings ϕ_i simultaneously. These two steps are repeated until an optimality condition is met.

The first step in the optimization of (6) requires repeated point-wise estimates of the mean metric structure and the "mean" mean curvature. While the curvature term is trivially computed, the first term has no closed-form solution. Iterative approximation is required. Under the log metric, the mean metric is a 2x2 matrix satisfying

$$G(g_S) = \arg \min_{g_S \in SPD(2)} \sum_i \left\| \operatorname{Log}\left[g_{S_i}^{-\frac{1}{2}} g_S g_{S_i}^{-\frac{1}{2}} \right] \right\|_F^2 . \quad (7)$$

The gradient of the above expression can be shown to be

$$\nabla G_{jk} = \sum_i 2tr \left[\operatorname{Log} X_i \, X_i^{-1} \frac{d}{d g_{S,jk}} X_i \right], \qquad X_i = g_{S_i}^{-\frac{1}{2}} g_S g_{S_i}^{-\frac{1}{2}} . \quad (8)$$

This formulation differs slightly from [17], but the means are in fact equivalent.

The second step in the optimization scheme of (6) requires an additional term to ensure that the spherical remappings ϕ_i remain in Φ_U, i.e. that they remain area-preserving. We use the same term as was done in [1]. The second optimization step then becomes very similar to the optimization problem in [1] summed over the surfaces in $\mathfrak{s}$. The only difference is the absence of the Gaussian curvature term, which, as we have shown, is not needed for a unique representation.

The overall optimization problem for finding Karcher means in the intrinsic shape framework can now be stated briefly as finding the optimal metric and curvature structure ν and spherical reparameterizations φ_i to minimize the following cost:

$$\mathcal{C}(\mathfrak{s}, \nu, \{\varphi_i\}) = \sum_{S_i \in \mathfrak{s}} \mathcal{L}^2(S_i, \nu) + R \int_{\mathbb{S}^2} (\log det[D\varphi_i])^2 d\mathbb{S}^2 . \quad (9)$$

5 Implementation Details

5.1 Optimization

We follow [1], using the spherical fluid framework to optimize (9) and compute the Karcher mean. As an initial step, all surfaces are spherically registered to a single target shape, exactly as in [1]. The point-wise metric and curvature mean map serves as the initial guess before group-wise registration. From this point, the only difference between [1] and this work is that the moving template metric + curvature field is updated at every iteration as the current point-wise mean. The average mean curvature is straight-forward, while the average metric tensors can be estimated quickly with a backtracking line search using the gradient in (8).

5.2 Surface Reconstruction

In [19], the authors propose to integrate the Gauss-Codazzi equations directly to reconstruct a surface from its conformal parameterization. As we do not compute explicit conformal maps, using this approach on the general metric tensor may be computationally challenging. Instead, we use a least-squares estimate that is a modification of the approach in [1]. As in [1], we rely on discrete differential geometry operators described in [20]. Suppose we have a spherical mesh $m = \langle V, E \rangle$, $|x| = 1\ \forall x \in V$, and g, H defined at each vertex in V, with an edge set E. The mesh representing an embedding in space, $\langle S(V), E \rangle$ minimizes the least-squares problems:

$$E_g = \sum_{xy \in E} \sqrt{\boldsymbol{A}(x)\boldsymbol{A}(y)} \left(\|Sx - Sy\| - L_{xy} \right)^2,$$
$$L_{xy} = \frac{1}{2}[(x-y)^T g(x)(x-y)]^{1/2} + \frac{1}{2}[(x-y)^T g(y)(x-y)]^{1/2} \tag{10}$$
$$E_H = \sum_{x \in V} \boldsymbol{A}(x) \left(\left\langle \left[\sum_{y \in N_1(x)} \frac{(\cot a_{xy} + \cot b_{xy})(Sx - Sy)}{4\boldsymbol{A}(x)} \right], \boldsymbol{n}(x) \right\rangle - H(x) \right)^2.$$

Here, $\boldsymbol{n}$ is the surface normal, $\boldsymbol{A}(x)$ is the area element, and a_{xy}, b_{xy} are angles opposite edge xy. The area element can be estimated from the spherical area element and $det(g)^{\frac{1}{2}}$. The cotangent weights in the estimated curvature operator themselves vary with the evolving mesh. However, when the initial guess is sufficiently close, e.g. when it is the Euclidean mean, fixing $\cot a_{xy} + \cot b_{xy}$ according to the metric generally does not affect the quality of the solution. To solve the system in (10), we must define a fixed frame. This can be done by computing the shape of an individual triangle based on the metric tensor alone, and fixing it in space. In practice, avoiding this step when the initial guess is sufficiently close does not affect the behavior of the optimization.

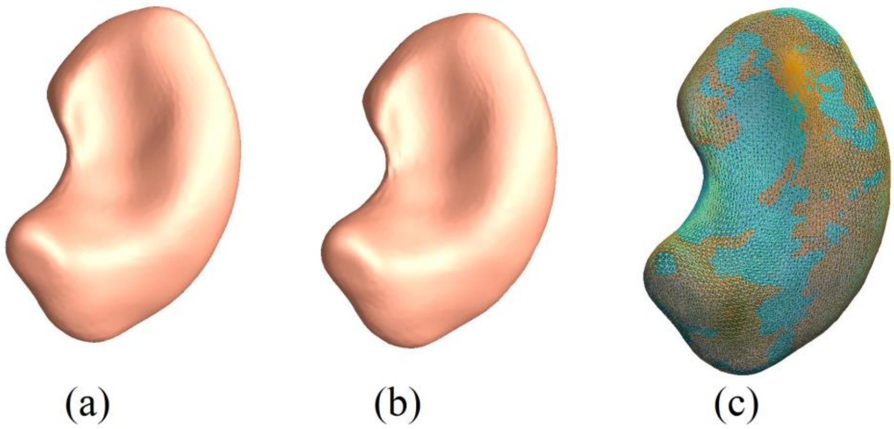

Fig. 2. Putamen (a) Euclidean mean; (b) Karcher mean; (c) overlay of (a) – blue and (b) – orange. Extreme curvatures are better preserved in Karcher means compared to Euclidean means consistently across shape types.

6 Experiments

We compute the Karcher means of 100 white matter surface models from healthy elderly participants in the ADNI 1 study. In **Figure 3**, we show the comparison to the Euclidean average. In general, more geometric detail is preserved over the Karcher mean, as Euclidean averaging tends to erode sharp features. Additional experiments were run on 400 subcortical shapes of typically developing children and young adults. Results for hippocampal shape are displayed in **Figure 4** and for putamen shape in **Figure 2**. Sum of squared distances $\sum_{S_i \in s} \mathcal{L}^2(S_i, \nu)$ is displayed in **Table 1** for the Euclidean and Karcher means. Compute times for the Karcher mean scale linearly with the number of subjects, since the reparameterization step is an order of magnitude costlier than the point-wise metric mean step of the optimization. When compared to the performance of pairwise registration in [1], the analogous computation here – a mean of two shapes – is not significantly different (on the order of a few minutes for a spherical harmonic bandwidth of 128).

Table 1. Sum of geodesic squares for Euclidean and Karcher means.

	Cortex	Hippocampus	Putamen
$\sum_{S_i \in s} \mathcal{L}^2(S_i, \nu)$ Euclidean	2.1 x 10^4	8.5 x 10^2	2.4 x 10^3
$\sum_{S_i \in s} \mathcal{L}^2(S_i, \nu)$ Karcher	5.4 x 10^3	3.2 x 10^2	1.4 x 10^3

7 Conclusion

We have presented a novel intrinsic shape representation in Riemannian setting, based on metric tensors and mean curvatures. In this setting, we show that it is possible to efficiently compute manifold mean representations and reconstruct their surfaces embedded in space. The mean estimation method is efficient due to the closed form solution for the geodesic length on the shape manifold. Our method is capable of group-wise registering complex shapes such as the cortical surface, and efficiently estimating sample means. When reconstructed into real surfaces, the realization of our mean estimate consistently preserves high-curvature and fine geometric features better than Euclidean averaging of coordinates. This provides some empirical proof that the suggested shape framework captures intrinsic properties of surfaces better than simpler methods based on the surface embedding.

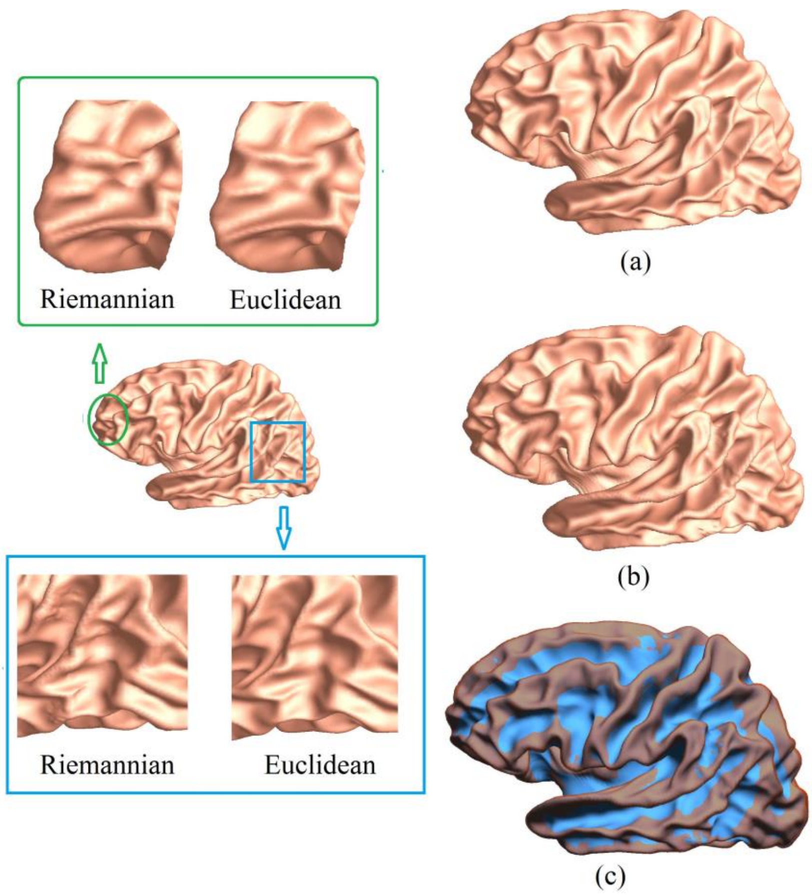

Fig. 3. (a) Euclidean Average; (b) Riemannian average – Karcher mean; (c) Overlay of (a) and (b), Karcher mean in orange, Euclidean mean in blue. Deeper sulci and taller gyri are prominent in the Riemannian average when compared to the Euclidean approximation.

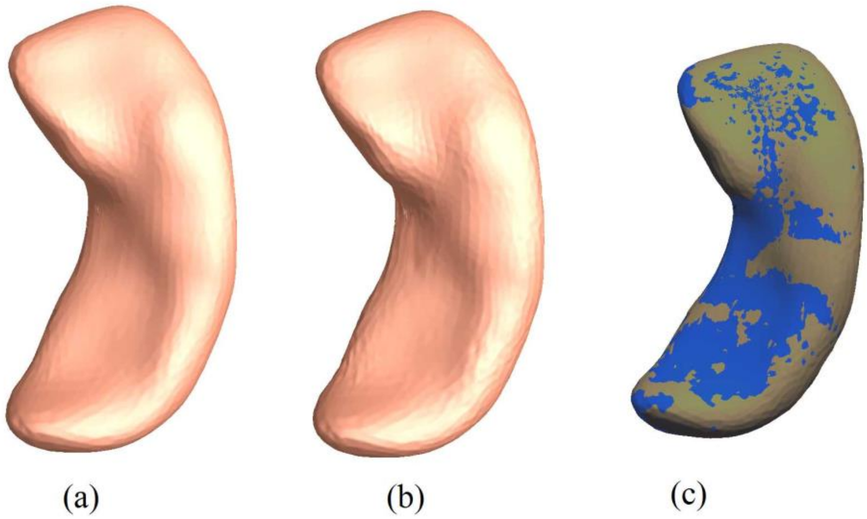

Fig. 4. Hippocampal (a) Euclidean mean; (b) Karcher mean; (c) overlay of (a) – blue and (b) – orange

References

1. Gutman, B.A., Fletcher, T.P., Cardoso, M.J., Fleishman, G., Lorenzi, M., Thompson, P.T., Ourselin, S.: A Riemannian Framework for Intrinsic Comparison of Closed Genus-Zero Shapes. Lect Notes Comput Sc (2015)
2. Gu, X., Wang, Y., Chan, T.F., Thompson, P.M., Yau, S.T.: Genus zero surface conformal mapping and its application to brain surface mapping. Ieee T Med Imaging 23, 949-958 (2004)
3. Zeng, W., Lui, L.M., Luo, F., Chan, T.F.-C., Yau, S.-T., Gu, D.X.: Computing quasiconformal maps using an auxiliary metric and discrete curvature flow. Numer. Math. 121, 671-703 (2012)
4. Shi, J., Thompson, P.M., Gutman, B., Wang, Y.: Surface fluid registration of conformal representation: Application to detect disease burden and genetic influence on hippocampus. Neuroimage 78, 111-134 (2013)
5. Yeo, B.T.T., Sabuncu, M.R., Vercauteren, T., Ayache, N., Fischl, B., Golland, P.: Spherical Demons: Fast Diffeomorphic Landmark-Free Surface Registration. Ieee T Med Imaging 29, 650-668 (2010)
6. Vercauteren, T., Pennec, X., Perchant, A., Ayache, N.: Diffeomorphic demons: Efficient non-parametric image registration. Neuroimage 45, S61-S72 (2009)
7. Gutman, B.A., Madsen, S.K., Toga, A.W., Thompson, P.M.: A Family of Fast Spherical Registration Algorithms for Cortical Shapes. In: Shen, L., Liu, T., Yap, P.-T., Huang, H., Shen, D., Westin, C.-F. (eds.) Multimodal Brain Image Analysis, vol. 8159, pp. 246-257. Springer International Publishing (2013)

8. Christensen, G.E., Rabbitt, R.D., Miller, M.I.: Deformable templates using large deformation kinematics. Image Processing, IEEE Transactions on 5, 1435-1447 (1996)
9. Yonggang, S., Rongjie, L., Wang, D.J.J., Pelletier, D., Mohr, D., Sicotte, N., Toga, A.W.: Metric Optimization for Surface Analysis in the Laplace-Beltrami Embedding Space. Medical Imaging, IEEE Transactions on 33, 1447-1463 (2014)
10. Bauer, M., Bruveris, M., Michor, P.: Overview of the Geometries of Shape Spaces and Diffeomorphism Groups. Journal of Mathematical Imaging and Vision 50, 60-97 (2014)
11. Qiu, A., Younes, L., Miller, M.I., Csernansky, J.G.: Parallel transport in diffeomorphisms distinguishes the time-dependent pattern of hippocampal surface deformation due to healthy aging and the dementia of the Alzheimer's type. Neuroimage 40, 68-76 (2008)
12. Bauer, M., Bruveris, M.: A new Riemannian Setting for Surface Registration. 3rd MICCAI Workshop on Mathematical Foundations of Computational Anatomy 182-194 (2011)
13. Ma, J., Miller, M.I., Younes, L.: A Bayesian Generative Model for Surface Template Estimation. International Journal of Biomedical Imaging 2010, 974957 (2010)
14. Kurtek, S., Klassen, E., Zhaohua, D., Jacobson, S.W., Jacobson, J.B., Avison, M.J., Srivastava, A.: Parameterization-Invariant Shape Comparisons of Anatomical Surfaces. Medical Imaging, IEEE Transactions on 30, 849-858 (2011)
15. Gu, X., Wang, Y., Yau, S.-T.: Geometric Compression Using Riemann Surface Structure. 171-182 (2003)
16. Ebin, D.G.: On the space of Riemannian metrics. 1001-1003 (1968)
17. Moakher, M.: A Differential Geometric Approach to the Geometric Mean of Symmetric Positive-Definite Matrices. SIAM Journal on Matrix Analysis and Applications 26, 735-747 (2005)
18. Lawson, J.H.B., Tribuzy, R.d.A.: On the mean curvature function for compact surfaces. 179-183 (1981)
19. Lui, L.M., Wen, C.F., Gu, X.F.: A Conformal Approach for Surface Inpainting. Journal of Inverse Problems and Imaging 7, 863-884 (2013)
20. Meyer, M., Desbrun, M., Schröder, P., Barr, A.: Discrete Differential-Geometry Operators for Triangulated 2-Manifolds. In: Hege, H.-C., Polthier, K. (eds.) Visualization and Mathematics III, pp. 35-57. Springer Berlin Heidelberg (2003)